31st Congress of the International Council of the Aeronautical Sciences
Belo Horizonte, Brazil; September 09-14, 2018

DESIGN PARAMETER STUDY OF DRONE BLADE CONSIDERING AEROACOUSTICS

Yoonpyo Hong*, Dongyeon Han*, Kwanjung Yee**
***Department of Mechanical & Aerospace Engineering, Seoul National University,**
****Department of Mechanical Engineering / Institute of Advanced Aerospace Technology, Seoul National University**

Keywords: *Drone Blade, Design Parameter Study, Aeroacoustics*

Abstract

On rising of the demand of multi-rotor drone, its drawbacks that it has a loud noise and low operation time stand out recently. Through designing the planform of drone blade, these shortcomings are expected to improve. In this paper, wave-shaped drone blades are considered. Horizontal wave, vertical wave, and sweep were applied to the drone blade to evaluate the effect of design parameters on performances. A hybrid CFD solver based on RANS and free wake model was used for the aerodynamic analysis. Farassat formulation 1A equation was used for the aeroacoustic analysis. Applying the vertical wave to drone blade improves hovering performance by reducing tip vortex effect. Concurrently, the fact that waveform remarkably changes blade's sectional load distribution proposes the possibility of noise reduction.

1 Introduction

Recently, the demand and supply of multi-rotor drones have increased widely including the private area. Among the various unmanned aerial vehicles, the multi-rotor drones are attracting attention due to the convenience of control and the ability to hovering flight. However, along with these advantages, the drawbacks such as low operation time and loud annoying noise are on the rise. Abundant studies to solve these problems have been conducted, but the consideration of the aeroacoustic problem is insufficient.

Gwak [1] has established a framework for noise reduction research by identifying the noise generation mechanism of the multi-rotor and performing the numerical experiment and verification of it. According to his research, in a multi-rotor type drone, various noise sources exist similar to the conventional helicopter. However, multi-rotor blades are usually very thin and have a small trailing edge thickness. Noise analysis should be done carefully considering these characteristics. Meanwhile, various types of research have been carried out to optimize the blade planform for noise reduction in the rotary blade field. [2] Among them, there is a study that when a wave-form blade is applied to a fan, the noise is substantially reduced because of the diminished blade-vortex interaction. [3] Based on these studies, the effect of wave type blades on drones are investigated in this study. The effects of various wave shapes on the aerodynamic and noise performance are considered by using a conventional drone blade as the baseline.

2 Computational Methods

2.1 Analyzer of Aerodynamics

For the drone blade aerodynamic analysis, hybrid Computational Fluid Dynamics (CFD) solver is used. This hybrid CFD solver yields the flow fields around the rotor blades by solving Reynolds-averaged Navier-Stokes (RANS) equations. In the wake region a certain distance from the blade, the induced velocity is calculated

using a free wake model. By applying the calculated induced velocity to the boundary conditions of the peripheral region of the blade, complex flow phenomenon around the tip can be captured accurately. At the same time, the calculation time can be effectively shortened than full CFD.

The governing equations were solved as follows. The spatial difference is based on Roe's flux difference splitting scheme and the Van Alvada flux limiter. The time difference is based on the LU-SGS time marching scheme. The SA-DES model is used as the turbulence model. The wake model used in this solver is the Vatistas vortex core model [8] with Bhagwat-Leishman core growth model [9]. A study by Bhagwat showed that a typical rotor blade has self-similarity at specific δ value. Therefore, in this study, the analytical model of the initial vortex core radius and the artificial viscosity parameter was modified to fit the drone blades.

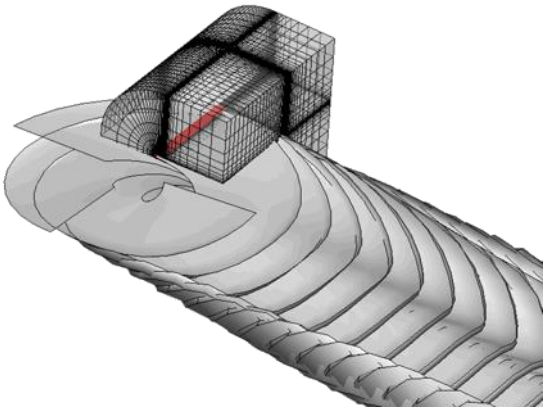

Figure 1 Concept of the hybrid CFD solver

2.2 Analyzer of Aeroacoustics

According to Gwak's research, noise sources of the drone blades are a discontinuous frequency noise and a broadband noise generated from the airfoil-self [1]. In order to predict the noise accurately, the prediction of the tone noise and the broadband noise should be performed together. However, the tone noise is only analyzed in this study because it is the most dominant noise source. Farassat formulation 1A, modified to facilitate the application of the Ffowcs–Williams & Hawkings (FW-H) equation to numerical experiment, is adopted for tone noise analysis [10]. The following expression shows the formulation 1A. In the expressions, p'_T and p'_L means a thickness noise and a loading noise, respectively.

$$4\pi p'_T(\boldsymbol{x},t) = \frac{\partial}{\partial t}\int_{f=0}\left[\frac{\rho_0 v_n}{r(1-M_r)}\right]_{ret} dS \quad (1)$$

$$4\pi p'_L(\boldsymbol{x},t) = \frac{1}{c}\frac{\partial}{\partial t}\int_{f=0}\left[\frac{pcos\theta}{r(1-M_r)}\right]_{ret} dS + \int_{f=0}\left[\frac{pcos\theta}{r^2(1-M_r)}\right]_{ret} dS \quad (2)$$

The thickness noise and the loading noise, which are major tone components from drone blades, can be predicted by these formulae. It can be seen from the equations that the thickness noise is caused by the Doppler effect as an object moving through a flow regardless of the pressure distribution on the surface. On the other hand, the loading noise is composed of the two terms. The first one is caused by the time-varying pressure on the blade surface. The other term is generated when a surface on which have constant pressure distribution has a relative velocity to a receiver, which is called Gutin noise.

Generally, drones have four or eight rotors, and there is an unsteady effect caused by uncertainties of the surrounding flow region in an actual flight. For a more accurate noise prediction result, the prediction of noise should be done considering all these effects. In this study, however, the effect of distance between the rotors of a drone can be neglected because a far-field receiver point is assumed. Also, a consideration of the unsteady effect caused by the uncertainty of the surrounding flow is limited, and the steady case is assumed because it increases the cost of the numerical analysis.

3 Design Parameter study

3.1 Definition of Design Parameters

The baseline drone blade used in the research is the KPROP, a drone made by Korea Aerospace Research Institute (KARI) [7]. This drone is composed of a conventional airfoil,

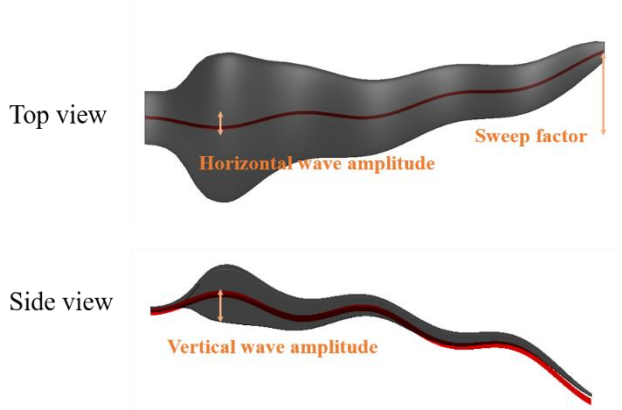

Figure 2 Design parameters of waveblade

SG6043, with proper twist distribution and tapered tip configuration. Based on KPROP blade, a parameter study was conducted by applying a wave shape to a vertical axis and horizontal axis.

The design parameters considered in this study are three: a horizontal wave amplitude, a vertical wave amplitude and a sweep factor. As shown in figure 2, the experimental blades have the same chord length and twist distribution with the baseline blade. The waveform is defined by a cosine function and a polynomial function. The exact formula is shown in Equation 3 and 4.

$$y=\alpha_1 \cos\left\{2n_w\pi\left(\frac{r}{R}\right)-\pi\right\}+\beta_1\left(\frac{r}{R}\right)^3 \quad (3)$$

$$z=\alpha_2 \cos\left\{2n_w\pi\left(\frac{r}{R}\right)-\pi\right\}+\beta_2\left(\frac{r}{R}\right)^3 \quad (4)$$

In these equations, α_1 and α_2 are the horizontal wave amplitude and the vertical wave amplitude factors, respectively. β_1 is a sweep factor, and β_2 has a fixed value of -0.002 for an anhedral configuration. n_w is the number of waves, and all blades have 3 waveforms. A total number of 12 sample blades are selected in this way, and they are shown in figure 3.

3.2 Results

Table 1 shows the operating conditions of drone blades considered in this study. In all cases, a trim analysis was carried out with the thrust by using rpm as a variable. The grid system for

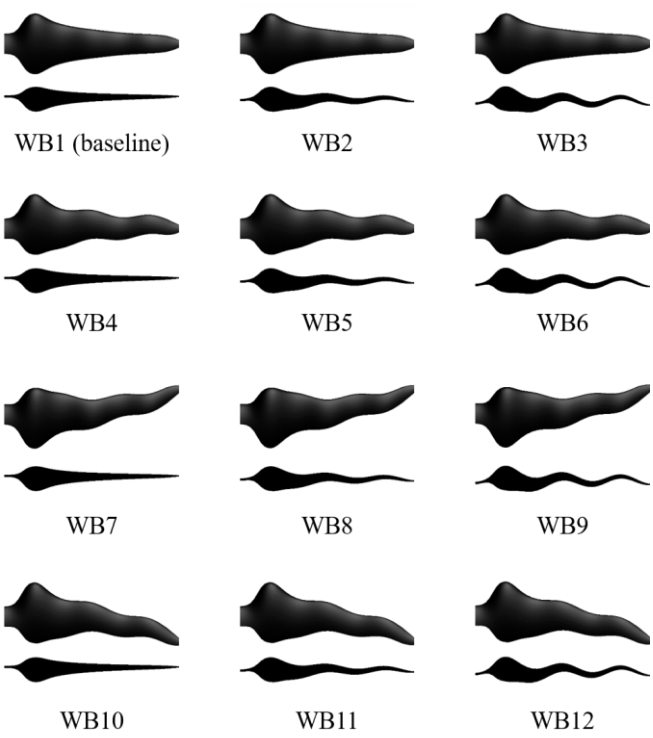

Figure 3 Planforms of waveblades

each blade was determined through a sensitivity test. The entire volume grid consists of 185 × 90 × 50 (chordwise × normal × spanwise) points, and surface grid consists of 137 × 90 (chordwise × spanwise) points.

Table 1 Operating conditions of baseline

Flight type	Hovering
RPM	4300
M_{tip}	0.37
Re_{tip}	86400
Thrust (N)	43.81

3.2.1 Aerodynamic Performance

The effect of the tip vortex is crucial for the entire multi-rotor drone performances, especially aerodynamic performance. The vertical wave of blade interferes with the development of tip vortex. The height difference due to the vertical wave near the tip generates radial velocity. This flow pushes the tip vortex outside, and the downwash from the vortex diminishes consequentially. The vertical wave also changes

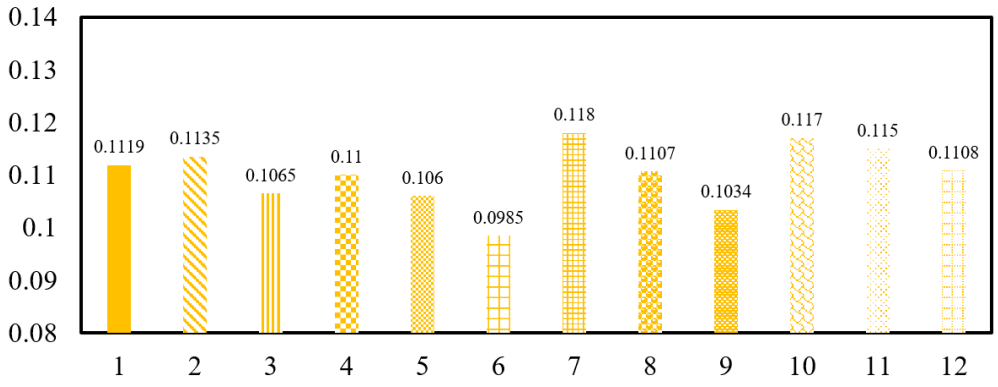

Figure 4 Vortex magnitude of the first vortex (normalized by tip speed and chord length)

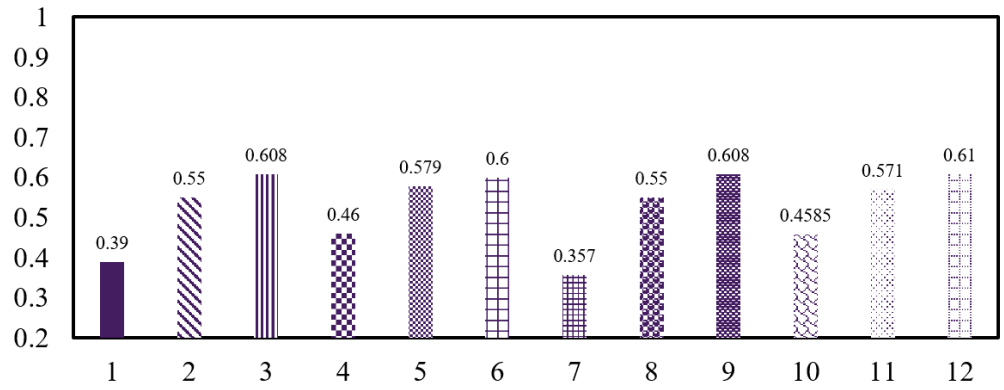

Figure 5 Vertical location of the first vortex (normalized by chord length)

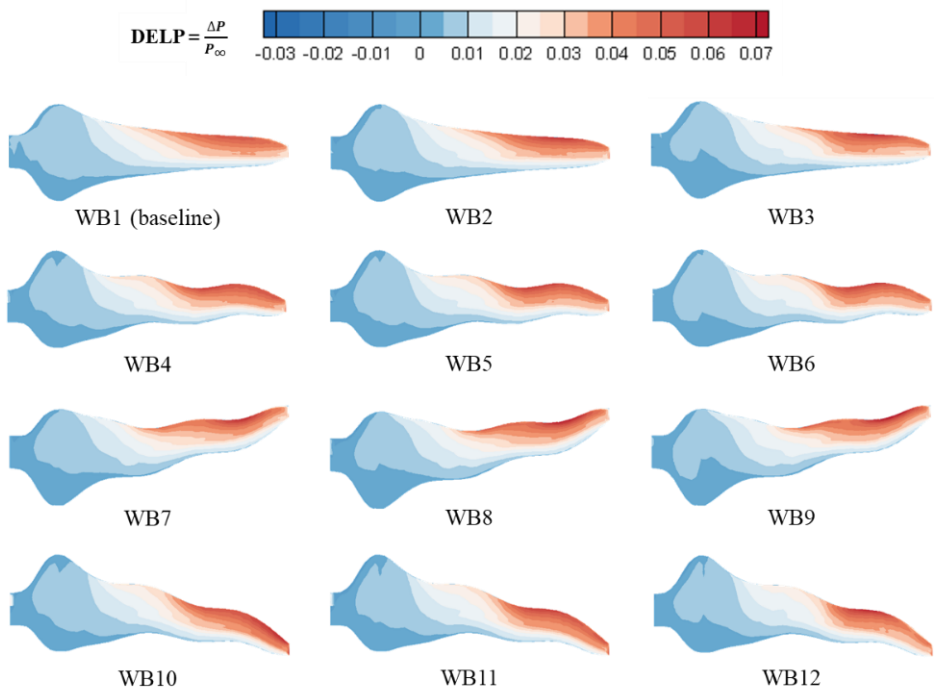

Figure 6 Pressure difference contour of waveblades (normalized by freestream pressure)

the generation position of the tip vortex. Figure 4 is a graph comparing the vortex magnitude of each blade and figure 5 shows the first vortex core location in the z-direction. From these two graphs, it can be seen that as the vertical wave amplitude increases, the vertical position of the

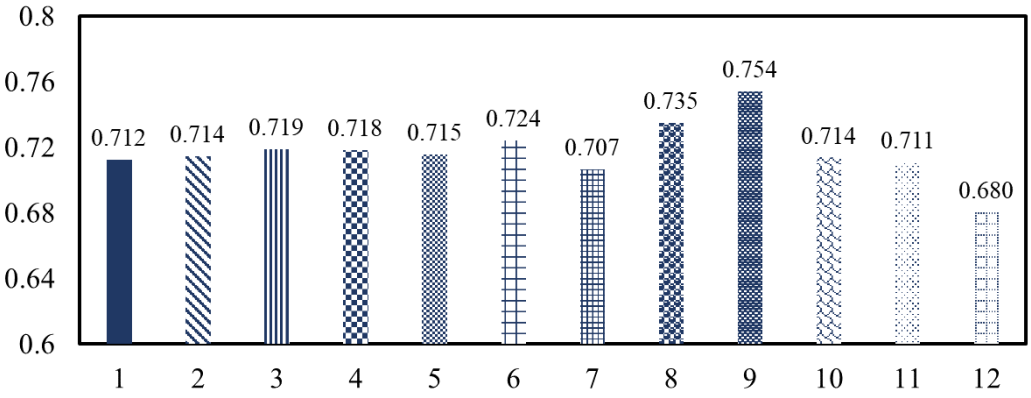

Figure 7 Figure of Merit of waveblades

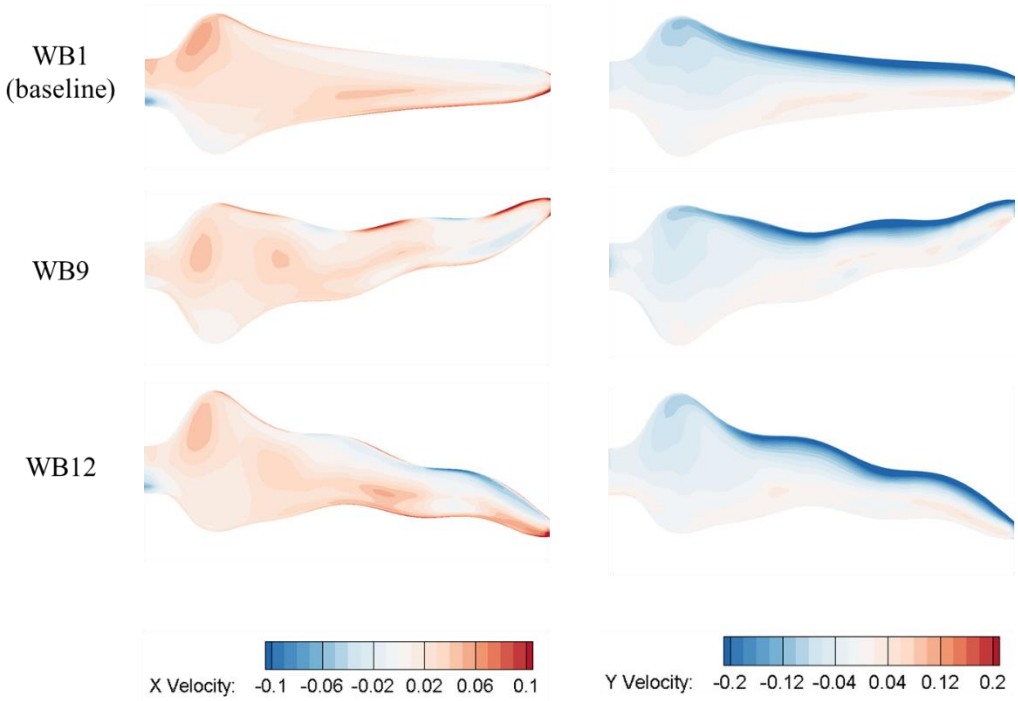

Figure 8 X & Y velocity contour on surfaces (normalized by a speed of sound) – WB1, WB9, WB12

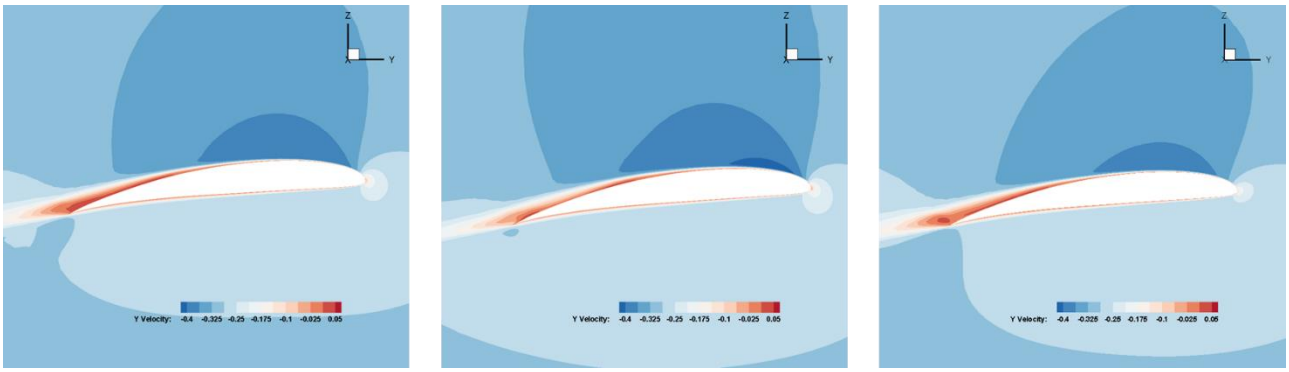

Figure 9 Y velocity contour at r/R = 0.95 (normalized by a speed of sound) - WB1, WB9, WB12

vortex core becomes lower and the vortex magnitude goes smaller.

Comparing the pressure difference contour on the blade in figure 6, the effect on the vertical wave amplitude is apparent. The portion of thrust

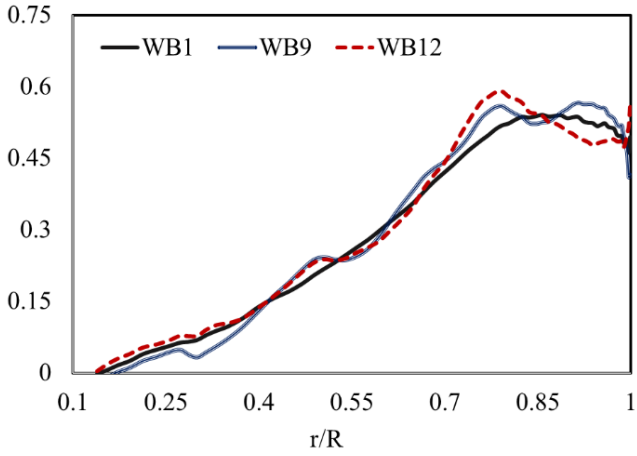

Figure 10 Sectional normal force coefficient distribution (WB1, WB9, WB12)

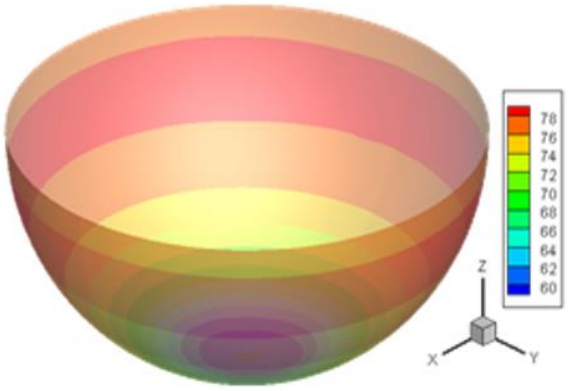

Figure 11 Shape of half sphere under rotor

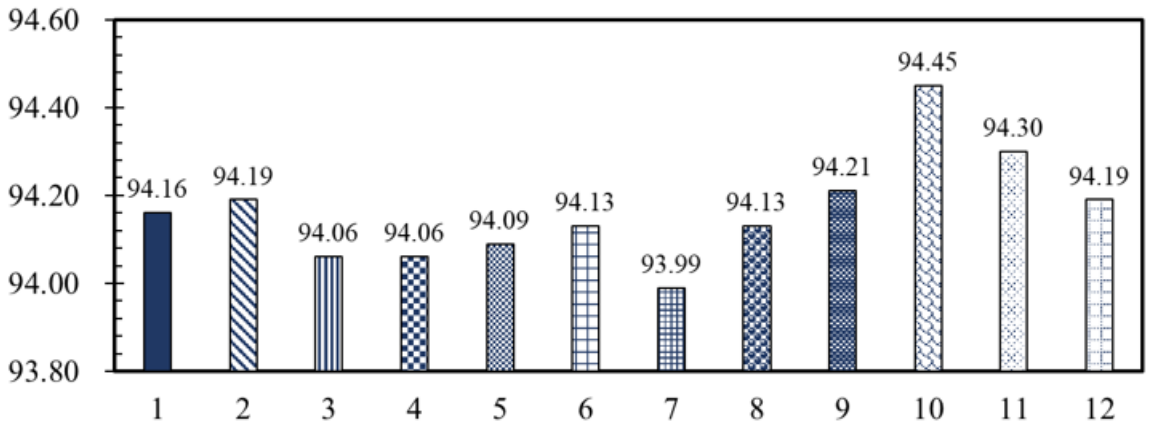

Figure 12 Half sphere power level (dB)

at the inboard side is larger as the higher amplitude of the vertical wave is applied to the blade. The area of the wave formed blade becomes relatively larger than baseline blade, and the inboard flux becomes abundant. This results in the reduced induced power.

The hovering efficiency, Figure of Merit (FM), of each blade is shown in figure 7. Sample blades have no significant change in FM with a comparison to the baseline blade except WB9 and WB12. Figure 8 shows the velocity contours of WB1, WB9, and WB12. The velocity is normalized by the speed of sound. As the flow has low Reynolds number and the angle of attack of drone blade is higher than those of conventional helicopter blade, the flow is detached near the trailing edge. Separation occurs from a spanwise section around r/R = 0.6 to the tip. The horizontal and the vertical waves affect this flow critically. In case of the WB9, a counter vortex is generated at the tip section due to the forward sweep shape, and it causes the outward radial flow. This flow gets stronger by the vertical wave effect, and the tip vortex weakens. Also, the counter vortex provides the energy to overcome adverse-pressure gradient and delays the separation. Therefore, thrust loss due to the separation diminishes. On the contrary, in the case of the WB12, the radial velocity due to horizontal wave has an opposite direction to the prior case because of the vertical wave. This weakens the outward radial velocity, and this invokes the opposite effect of WB9. Figure 9 shows the y velocity of WB1, WB9, and WB12 at r/R = 0.95. At the tip region, the separation of WB9 diminishes and that of WB12 increased as expected. Figure 10 shows the sectional normal force distribution of WB1, WB9, and WB12. The result of the above physical phenomenon appears as sectional normal force distribution.

3.2.2 Aeroacoustic Performance

The thickness noise is very small and the loading noise is dominant when the tip mach number is small like the case of drones. If several rotors steadily produce the same thrust, the loads on each rotor by the surrounding flow is similar. It means that the power levels of the noise radiated from each rotor is similar, too. Thus, the difference between the power levels of each rotor cannot be large unless there is an additional unsteady pressure perturbation. This can be explained by the expression for the loading noise prediction. The first term of the equation 2 has a partial derivative with respect to time, which results in a substantial value if the surface pressure field varies significantly with the azimuth angle of the blade. On the other hand, in the case of the second term, there is no consideration of the change in time, which is a loading noise due to the Doppler effect of the steady pressure field on the blade surface. That is, regardless of the state of the pressure field on the blade surface, the second term contributes to the loading noise. Uncertain unsteady pressure field can increase the magnitude of the first term, and the loading noise can be grown up by this unsteadiness.

In this study, the unsteady effect of the aerodynamics is not significant because the operating conditions of the drones are limited to the hovering flight which is the most frequent flight condition of drones. Thus, the difference of the power level radiated from the different rotor cannot be remarkably large. The figure 11 and 12 show an under-rotor spherical surface and the power level of the noise radiated to the surface respectively.

As shown in figure 12, the scale of the graph is dense so that the difference of the power levels of each blade is very small, within 1 dB . However, there are two blades, WB7 and WB10, which have relatively large difference between them. The result of comparing the noise level of the blades with the WB4 is shown in figure 13. The graph shows that the difference of the noise level of each blade is prominent from the rotor surface to the lower side of 45°, and similar noise levels are observed thereafter. As mentioned before, the noise component which has a dominant influence on the noise level is the loading noise, and the larger the load acting on the tip, the higher the noise level can be generated.

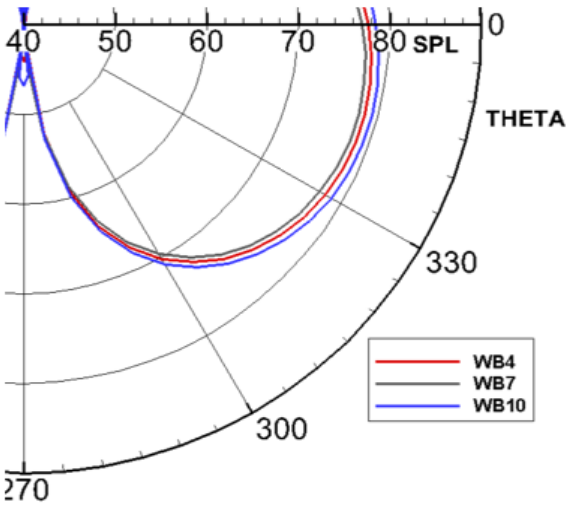

Figure 13 Sound Pressure Level (dB) under rotor surface

4 Concluding Remarks

Aerodynamic and aeroacoustic characteristics of the modified multi-rotor type drone blades that have wave-shaped planforms were considered. The 12 test blades were formed with 3 design parameters: horizontal wave amplitude, vertical wave amplitude and sweep factor. The conclusion of this study is as follows.

1. The vertical wave makes the height differences on the whole blade and radial flow. Among them, the difference at tip region brings the outward direction radial flow and make the tip vortex weak. Also, the formation of tip vortex become lower due to the vertical wave. This results in diminished tip vortex effect and an increase in hovering flight efficiency.

2. Horizontal wave and sweep planform make radial velocity like as vertical wave. In case of the WB7~9, forward sweep planform at tip region causes the counter vortex and outward radial flow. Especially in case of WB9, two radial flow by the vertical wave and horizontal wave make the effect of tip vortex weak. Also, the counter vortex provides energy to delay the separation near

the tip region. On the other hand, the WB12 reverses the direction of the two velocities, and it results in adverse effects.

3. Although there is a limitation that only discontinuous frequency noise is analyzed in this study, the results of the parametric study show that a tendency exists. All blades have the same twist and chord length distribution in the spanwise direction, the sectional normal force distribution is different. This means a significant change in load could be generated at the tip region. It is confirmed that the tendency of the load at the tip and the noise level coincide with each other. In conclusion, by using these characteristics, design optimization of the drone blade for aerodynamic and aeroacoustic performance could be done as future work.

Acknowledgement

This research was conducted at High-Speed Compound Unmanned Rotorcraft (HCUR) research laboratory with the support of Agency for Defense Development (ADD).

References

[1] Gwak D. Analysis and Prediction of Sound Quality Factors influencing Annyance from UAV noise. Ph.D Dissertation, Dept. of Mechanical and Aerospace Engineering, Seoul National University, Seoul, Korea, 2017.
[2] Brocklehurst A and Barakos G.N. A review of helicopter rotor blade tip shapes. Progress in Aerospace Sciences, Vol. 56, pp 35-74, 2013.
[3] Cho K. Assessment of Aerodynamic Noise Generation Mechanism and its Reduction in Axial Flow Fan. Ph.D Dissertation, Dept. of Mechanical and Aerospace Engineering, Seoul National University, Seoul, Korea, 2003.
[4] Lee J and Yee K. Improvement of Computational Efficiency for Rotor Flowfield Analysis Using Computational-Fluid-Dynamics-Free-Wake Coupling Method. Journal of Aircraft, Vol. 53, No. 6, pp 1953-1958, 2016.
[5] Yoon S, Ventura D, Boyd D, Chan W, and Theodore C. Computational Aerodynamic Modeling of Small Quadcopter Vehicles. The 73rd Annual AHS International Forum & Technology Display, Fort Worth, Texas, May 2017.
[6] Ramasamy M, Lee T and Leishman J. Flowfield of a Rotating-Wing Micro Air Vehicle. Journal of Aircraft, Vol.44, No.4, pp 1236-1244, 2007.
[7] Wie S, Kang H, Kim T, Kee Y, and Song J. High-efficiency propeller development for Multicopter type UAV. Journal of the Korean Society for Aeronautical & Space Sciences, Vol.45, No.7, pp 581-593, 2017.
[8] Vatistas G. New Model for Intense Self-Similar Vortices. Journal of Propulsion and Power, Vol. 14, No. 4, pp 462-469, 1998.
[9] Bhagwat M, and Leishman J. Generalized Viscous Vortex Model for Application to Free-vortex Wake and Aeroacoustic Calculations. The 58th Annual AHS International Forum, 2002.
[10] Farassat F. Derivation of Formulations 1 and 1A of Farassat. NASA Technical Memorandum, No.214853, 2007.

Contact Author Email Address

Kwanjung Yee
Email : kjyee@snu.ac.kr

Copyright Statement